

David Bracco, Daniel Thiébaud, René L. Chioléro, Michel Landry, Peter Burckhardt and Yves Schutz
J Appl Physiol 81:2580-2587, 1996.

You might find this additional information useful...

This article has been cited by 10 other HighWire hosted articles, the first 5 are:

Current state of bioimpedance technologies in dialysis

P. Kotanko, N. W. Levin and F. Zhu

Nephrol. Dial. Transplant., March 1, 2008; 23 (3): 808-812.

[Full Text] [PDF]

Applicability of a segmental bioelectrical impedance analysis for predicting the whole body skeletal muscle volume

N. I. Tanaka, M. Miyatani, Y. Masuo, T. Fukunaga and H. Kanehisa

J Appl Physiol, November 1, 2007; 103 (5): 1688-1695.

[Abstract] [Full Text] [PDF]

Modeling upper and lower limb muscle volume by bioelectrical impedance analysis

A. Stahn, E. Terblanche and G. Strobel

J Appl Physiol, October 1, 2007; 103 (4): 1428-1435.

[Abstract] [Full Text] [PDF]

Applicability of segmental bioelectrical impedance analysis for predicting trunk skeletal muscle volume

N. Ishiguro, H. Kanehisa, M. Miyatani, Y. Masuo and T. Fukunaga

J Appl Physiol, February 1, 2006; 100 (2): 572-578.

[Abstract] [Full Text] [PDF]

Segment-specific resistivity improves body fluid volume estimates from bioimpedance spectroscopy in hemodialysis patients

F. Zhu, M. K. Kuhlmann, G. A. Kaysen, S. Sarkar, C. Kaitwatcharachai, R. Khilnani, L. Stevens, E. F. Leonard, J. Wang, S. Heymsfield and N. W. Levin

J Appl Physiol, February 1, 2006; 100 (2): 717-724.

[Abstract] [Full Text] [PDF]

Medline items on this article's topics can be found at <http://highwire.stanford.edu/lists/artbytopic.dtl> on the following topics:

Medicine .. Absorptiometry/Bone Densitometry

Medicine .. X-Ray Densitometry

Medicine .. Obesity

Medicine .. Body Composition

Medicine .. Obese Women

Physiology .. Humans

Updated information and services including high-resolution figures, can be found at:

<http://jap.physiology.org/cgi/content/full/81/6/2580>

Additional material and information about *Journal of Applied Physiology* can be found at:

<http://www.the-aps.org/publications/jappl>

This information is current as of December 1, 2009 .

Segmental body composition assessed by bioelectrical impedance analysis and DEXA in humans

DAVID BRACCO, DANIEL THIÉBAUD, RENÉ L. CHIOLÉRO, MICHEL LANDRY, PETER BURCKHARDT, AND YVES SCHUTZ
Institute of Physiology, Faculty of Medicine, University of Lausanne and Departments of Surgical Intensive Care, Internal Medicine, and Radiology, University Hospital, CH-1011 Lausanne, Switzerland

Bracco, David, Daniel Thiébaud, René L. Chioléro, Michel Landry, Peter Burckhardt, and Yves Schutz. Segmental body composition assessed by bioelectrical impedance analysis and DEXA in humans. *J. Appl. Physiol.* 81(6): 2580–2587, 1996.—The present study assessed the relative contribution of each body segment to whole body fat-free mass (FFM) and impedance and explored the use of segmental bioelectrical impedance analysis to estimate segmental tissue composition. Multiple frequencies of whole body and segmental impedances were measured in 51 normal and overweight women. Segmental tissue composition was independently assessed by dual-energy X-ray absorptiometry. The sum of the segmental impedance values corresponded to the whole body value ($100.5 \pm 1.9\%$ at 50 kHz). The arms and legs contributed to 47.6 and 43.0%, respectively, of whole body impedance at 50 kHz, whereas they represented only 10.6 and 34.8% of total FFM, as determined by dual-energy X-ray absorptiometry. The trunk averaged 10.0% of total impedance but represented 48.2% of FFM. For each segment, there was an excellent correlation between the specific impedance index ($\text{length}^2/\text{impedance}$) and FFM ($r = 0.55, 0.62,$ and 0.64 for arm, trunk, and leg, respectively). The specific resistivity was in a similar range for the limbs (159 ± 23 cm for the arm and 193 ± 39 cm for the leg at 50 kHz) but was higher for the trunk (457 ± 71 cm). This study shows the potential interest of segmental body composition by bioelectrical impedance analysis and provides specific segmental body composition equations for use in normal and overweight women.

dual-energy X-ray absorptiometry; body segments; body fat; fat-free mass

ASSESSMENT OF BODY COMPOSITION plays an important role in nutritional evaluation, and bioelectrical impedance analysis (BIA), which has been known for more than 50 years, has become widely used in clinical settings during the last 10 years (10, 13, 14). Numerous investigations have demonstrated the usefulness of BIA in assessing body composition, body composition changes, and body fluid distribution in a wide range of physiological and clinical conditions (6, 11, 19). The resistance of tissues to electrical current is directly related to their fluid content: the highly hydrated fat-free mass (FFM) is a good electrical conducting medium, whereas the poorly hydrated adipose tissue is a good electrical insulator. In normal and ill subjects, BIA is correlated with total body water, and the variations of both are also correlated (11). Measurements of the conducting volume of the body is based on Ohm's law, which states that a volume of constant section is proportional to the length squared (L^2) divided by its resistance. However, recently, growing interest has

focused on certain limitations of this method, such as the geometry of the measured conductor: there is a linear relationship between bioelectrical impedance index ($\text{height}^2/\text{resistance}$) and FFM, provided the conductor measured is apperanted to a cylinder or has a constant section. This is obviously not the case when assessing the whole body BIA, as the conductor usually measured (wrist to ankle) consists of two long thin conductors (limbs) separated by a shorter and thicker one (trunk). Despite this limitation, most investigators have demonstrated a good relationship between the square of index height-to-whole body resistance and FFM (11), since the relative contribution of each segment increases in concert with body size.

The aims of the present study were to 1) describe segmental body composition by segmental BIA and dual-energy X-ray absorptiometry (DEXA), 2) analyze the relationship in healthy subjects between segmental FFM by BIA and DEXA, and 3) determine the relationships between the $L^2/\text{impedance}$ index and the segmental FFM for each segment at three different frequencies.

METHOD

Subjects. The study was carried out at the Institute of Physiology and the Radiology Department of the University Hospital of Lausanne. Subjects were recruited among medical students of the University and among women channeled to the Institute of Physiology for nutritional and metabolic evaluations. The study is in accordance with the Declaration of Helsinki, and the protocol was approved by the Ethical Committee of the Faculty of Medicine of the University of Lausanne. The study sample consisted of 51 women without any medication and without known disease except for obesity, ranging in age from 18 to 62 yr and ranging in body weight from 48.6 to 131.2 kg. On a random basis, two-thirds of the subjects ($n = 34$) were assigned to the equation-prediction group and 17 subjects were in the validation group.

Anthropometry. After an overnight fast and after voiding, the subjects' body weight in minimal clothing (underwear and brassiere) was measured to the nearest 100 g with a precision scale and height was measured to the nearest 5 mm with a Holtain stadiometer. An anthropometric evaluation was performed by triplicate skinfold thickness measurement at four sites (biceps, triceps, subscapular, and supra iliac) with a Harpenden caliper (7). The lengths of the arm, trunk, and leg were precisely measured between the center of the impedance electrodes. Anthropometric assessment was completed with waist, hip, bicipital, and wrist circumferences. To avoid interinvestigator variability, anthropometric evaluation was performed by two trained investigators (Y. Schutz and D. Bracco).

BIA. Whole body and segmental bioelectrical impedance were recorded on the right side of the body by using a portable

device built by the Electronic Department of the University Hospital (26). The device measures the resistance and the reactance at 0.5, 50, and 100 kHz after injecting a 500- μ A current from the wrist to the ankle (26). This electrical current is below the threshold for sensibility and is \sim 40% lower than most commercially available BIA devices, which inject 800 μ A to subjects. Current-injecting electrodes, located at the external side of the wrist and the ankle, were left in place for the entire investigation. Four ungelled sensing electrodes were placed after cleaning the skin with a 50% ethanol solution. The precise location of these electrodes were 1) the anterior part of the wrist 2 cm proximal to the radial process, 2) over the center of the anterior face of the humeral head, 3) over the anterior-superior iliac spine, and 4) over the internal malleolus. Whole body impedance was measured between the wrist and ankle, and segmental impedance was measured between the two nearby electrodes (Fig. 1). This configuration allows measurements of the whole body and segmental impedance while keeping the current-injecting electrodes at the same place, thus not influencing the electrical current across the body. Measurements were done while the subjects were lying on a nonconducting surface and with the limbs abducted from the trunk so that the medial parts of the limbs did not contact the trunk or each other. Electrode configuration is somewhat comparable to the previously described segmental BIA studies (1, 4, 5, 8, 9, 18). Segments measured correspond to *segments 1, 4, and 18* of the study recently published by Organ et al. (18). The impedance of the trunk was measured with the subjects breathing quietly, and the average resistance and reactance over the respiratory cycle were recorded. Whole body and segmental resistance and reactance were measured in triplicate, and if the difference between the three readings was $>3 \Omega$, the measurement was repeated. Whole body and segmental resistance and reactance were measured, and impedance and phase angle were calculated from the vectorial resultant of these two components.

DEXA. DEXA (model QDR 2000, Hologic) was used to assess body composition independently. Subjects were measured while wearing only a standard light cotton shirt to minimize clothing absorption. Measurements were performed by a trained radiology technician with dual-energy

X-ray beams at 70 and 140 KeV. Single rectilinear scanning mode was used on a 148×330 pixel matrix in a 196×80 cm window. Although DEXA was the first method developed to measure bone mineral density (15), the application to whole body soft tissue composition has become current practice (20). The DEXA device measures the attenuation of the two energy X-ray beams crossing the tissue. This allows partitioning between bone vs. soft tissue and fat vs. lean tissue in pixels of the body where there is no overlying calcified tissue. The DEXA device provides for each area the mass of bone, soft tissue FFM, and fat. For further computations and comparison with BIA, FFM including bone mineral content (also taken into account by the BIA method) was taken. The duration of total body scanning time was 15 min, and total X-ray irradiation absorbed by the organism was <5 mrem, which corresponds to 10% of a standard chest film. Total body scanning area was divided into precise anatomic segments: the arms were separated from the trunk by a line passing through the humeral head and the apex of the axilla. The trunk was separated from the legs by a line passing from the iliac crest to the perineum. The head was excluded from the trunk by a horizontal line passing just below the mandible. The use of precise identical anatomic landmarks in both BIA and DEXA allowed the comparison of these two methods.

Computations. Computation methods underlying the BIA technique are reviewed elsewhere (11) and demonstrate that there is a linear relationship between FFM and the L^2 /impedance index

$$\text{FFM} = \frac{\text{length}^2}{\text{resistance}} \times \text{constant} \quad (1)$$

For high-frequency currents (≥ 50 kHz), the conducting volume is assumed to represent the highly hydrated lean tissue (i.e., FFM) of the analyzed segment, whereas low-frequency currents flow mainly through the extracellular volume (27).

By using this approach, specific resistivity can be estimated from 1) FFM independently derived from DEXA, 2) length measured by anthropometry, and 3) impedance measured by BIA

$$\text{specific resistivity} = \frac{\text{FFM} \times \text{resistance}}{\text{length}^2 \times 1.1} \quad (2)$$

where 1.1 represents the specific gravity of FFM (g/ml).

Statistical analysis. Data were analyzed by using a statistical package of SAS Institute with parametric tests (25). In the prediction group, linear regression analyses were used for comparing FFM and the L^2 /resistance index. In the validation group, the bias was calculated for each subject by using the Bland and Altman technique (2). For comparison with the other studies, data from the prediction and validation groups were pooled. All results are expressed as means \pm SD, and $P < 0.05$ is considered statistically significant.

RESULTS

Anthropometry. As shown in Table 1, the sample studied purposely covered a broad range of body weight, ranging from lean to morbidly obese. However, as in current population studies, the sample showed a slight kurtosis toward high body weight, since markedly overweight subjects were also included. This is illustrated by the fact that median body weight (71.5 kg), body mass index (BMI; 23.9 kg/m^2), and percentage or ideal body weight (109%) were lower than their respec-

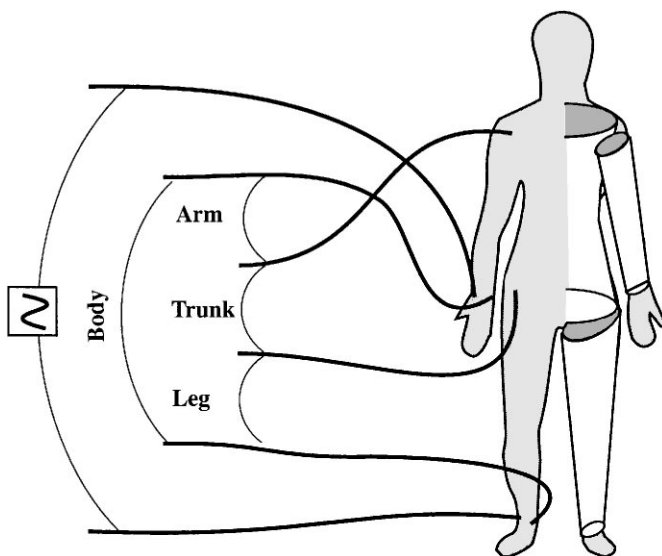


Fig. 1. Experimental setup. Whole body and segmental impedances were measured, keeping current-injecting electrodes at same anatomic location. The body can be considered to be 2 thin long conductors separated by shorter and thicker conductor.

Table 1. Anthropometric characteristics of subjects

	Prediction Group	Validation Group	Global Sample	
Anthropometry				
Weight, kg	74.5 ± 3.9	77.1 ± 5.4	75.3 ± 3.1	(48.6–131.2)
Height, cm	165 ± 1	166 ± 1	165 ± 1	(153–175)
Age, yr	33 ± 2	28 ± 3	31 ± 2	(18–62)
Sum of 4 skin-folds, mm	86 ± 9	84 ± 13	85 ± 7	(22–174)
Body mass index, kg/m ²	27.5 ± 1.5	28.3 ± 2.1	27.8 ± 1.2	(17.0–52.6)
%Ideal body weight	130 ± 7	133 ± 10	131 ± 6	(81–247)
DEXA				
Derived body weight, kg	74.3 ± 3.6	76.6 ± 6.1	75.1 ± 3.1	(47.2–127.7)
Whole body FFM, kg	45.6 ± 0.7	45.9 ± 1.2	45.7 ± 0.6	(38.8–55.2)
Whole body fat, kg	28.7 ± 3.2	30.8 ± 5.2	29.4 ± 2.7	(3.8–73.6)
%Body fat by DEXA	35.1 ± 2.4	35.9 ± 3.6	35.4 ± 2.0	(7.4–60.6)
Arm FFM, kg	2.13 ± 0.06	2.06 ± 0.07	2.11 ± 0.05	(1.61–3.50)
Arm fat, kg	1.90 ± 0.21	2.02 ± 0.38	1.94 ± 0.19	(0.26–5.75)
Arm length, cm	50.7 ± 0.4	52.4 ± 7.7	51.2	(46.5–61.0)
Trunk FFM, kg	23.3 ± 0.4	23.0 ± 0.5	23.2 ± 0.36	(19.3–31.6)
Trunk fat, kg	13.1 ± 1.8	13.5 ± 2.7	13.2 ± 1.5	(0.4–37.2)
Trunk length, cm	45.9 ± 0.6	45.8 ± 1.0	45.8 ± 0.5	(40.5–55.0)
Leg FFM, kg	7.16 ± 0.12	7.49 ± 0.29	7.27 ± 0.12	(5.82–10.41)
Leg fat, kg	5.51 ± 0.51	6.19 ± 0.96	5.74 ± 0.47	(1.10–15.01)
Leg length, cm	81.1 ± 0.9	85.0 ± 8.8	82.4 ± 0.7	(58.0–90.0)

Values are means ± SD with ranges in parentheses. $n = 34, 17$, and 51 subjects in prediction group, validation group, and global sample, respectively. FFM, fat-free mass; DEXA, dual-energy X-ray absorptiometry.

tive mean values. Prediction and validation groups were comparable in terms of weight, height, age, BMI, and body composition.

DEXA. Body composition assessment by DEXA demonstrated an excellent agreement between measured body weight and reconstituted weight from the sum of all DEXA pixels. The bias was <1 kg for both groups (mean absolute weight difference of 0.74 ± 0.67 kg). There was also a good correlation between left and right limb FFM, the mean absolute difference in segmental FFM being only 180 ± 270 g (not significant) for the arms and 180 ± 160 g (not significant) for the legs, confirming the precision of segments delineation by the radiology technicians. The limbs showed a tendency to a higher percentage of fat ($42.7 \pm 14.9\%$ for arms and $41.0 \pm 12.1\%$ for legs) compared with the trunk ($31.4 \pm 16.9\%$). From the leanest to the most overweight women, relative body fat increased more in the trunk (1.5–62.1%) than in the arm (9.9–68.5%) or the legs (14.3–63.5%). The contribution of each segment to increasing body weight is illustrated in Fig. 2, which shows the segmental composition of the 51 women ranked by increasing weight (from 48.6 to 131.2 kg). Whole body FFM increased twofold from 38.8 to 55.2 kg, whereas fat mass increased a 20-fold range, i.e., from 3.8 to 73.6 kg. The major part of this fat accumulation occurred in the trunk, where fat mass increased by a factor of one hundred (from 0.4 to 37.2 kg). From the regression

coefficient between fat mass and weight ($r^2 = 0.97$, $P < 0.0001$), it could be calculated that for each kilogram of change in weight the relative contribution of fat to the additional weight was as high as 86%. The FFM rose only slightly with increasing obesity, and the major part of adipose tissue deposition occurred in the trunk. The change in the composition of the limbs was less marked. From the slopes of the regression lines, we can establish that 1 kg of additional weight contains 127 ± 22 g FFM ($r = 0.64$, $P < 0.0001$), 466 ± 14 g fat deposited in the trunk ($r = 0.98$, $P < 0.0001$), 288 ± 12 g fat in the legs ($r = 0.96$, $P < 0.0001$), and 102 ± 10 g fat in the arms ($r = 0.85$, $P < 0.0001$).

Segmental body composition by impedancemetry. BIA (Table 2) confirmed that the major part of body impedance at the three measured frequencies (0.5, 50, and 100 kHz) was confined to the limbs, with the trunk constituting only a small part of the total whole body bioelectrical impedance. There was an excellent recovery between the measured whole body resistance and reactance (wrist to ankle) and the sum of the segmental BIA measurements. However, this was not the case for 0.5-kHz reactance, secondary to the fact that the measured values were close to zero (95% of values <10 Ω for whole body). Given the precision of our instrument (± 1 Ω) and the possible dielectric capacitive effect at the level of the skin surface with such low frequencies, recoveries of >100% may not be surprising.

Derived equations for segmental body composition by BIA. On a physiological-mathematical basis, the $L^2/$

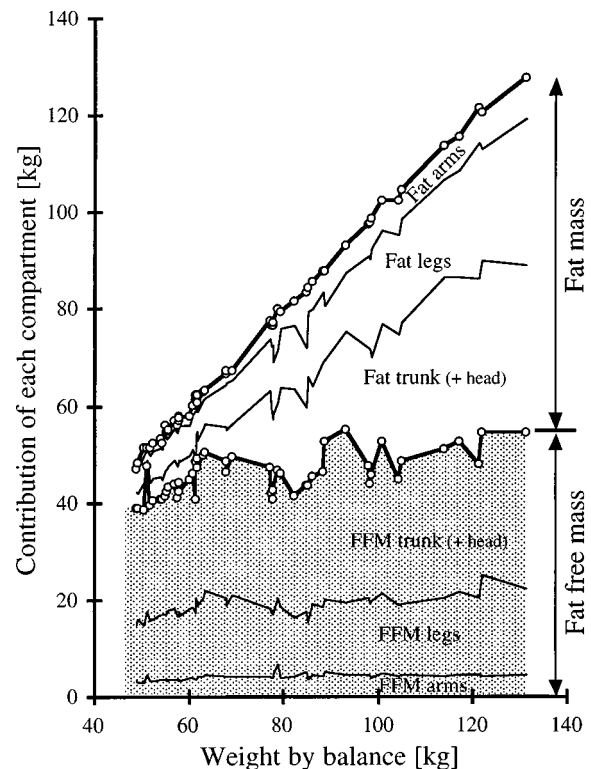


Fig. 2. Contribution of each body segment to body composition as measured by dual-energy X-ray absorptiometry (DEXA). Women studied ($n = 51$) were ranked by increasing body weight (by scale). FFM, fat-free mass.

Table 2. Segmental body composition analysis by BIA

	Body	Arm	Trunk	Leg	Sum	%Body
Resistance, Ω						
500 Hz	568 \pm 67	267 \pm 39	57 \pm 6	253 \pm 32	573 \pm 68	100.9 \pm 1.4
50 kHz	460 \pm 57	221 \pm 36	45 \pm 6	196 \pm 25	463 \pm 57	100.5 \pm 1.9
100 kHz	422 \pm 51	208 \pm 33	40 \pm 5	176 \pm 22	424 \pm 52	100.4 \pm 1.9
Reactance, Ω						
500 Hz	5 \pm 3	2 \pm 2	2 \pm 1	6 \pm 3	10 \pm 4	259 \pm 303
50 kHz	78 \pm 13	31 \pm 8	10 \pm 3	37 \pm 6	75 \pm 14	99.9 \pm 7.8
100 kHz	89 \pm 19	28 \pm 11	10 \pm 3	46 \pm 6	85 \pm 19	94.8 \pm 6.3
Impedance, Ω						
500 Hz	568 \pm 67	263 \pm 39	46 \pm 6	254 \pm 32	573 \pm 68*	100.9 \pm 1.4
50 kHz	467 \pm 58	223 \pm 36	41 \pm 5	200 \pm 25	470 \pm 58*	100.5 \pm 1.9
100 kHz	432 \pm 53	210 \pm 34	41 \pm 5	182 \pm 23	432 \pm 53*	100.1 \pm 1.8
Impedance, %whole body impedance						
500 Hz		46.1 \pm 2.7	10.1 \pm 1.3	44.7 \pm 2.7		
50 kHz		47.6 \pm 3.1	10.0 \pm 1.4	43.0 \pm 2.9		
100 kHz		48.6 \pm 3.3	9.6 \pm 1.3	42.2 \pm 3.1		
Phase, $^\circ$						
500 Hz	0.5 \pm 0.3	0.6 \pm 0.6	2.0 \pm 1.7	1.3 \pm 0.7	1.0 \pm 0.4 \dagger	
50 kHz	9.8 \pm 1.1	8.1 \pm 1.7	11.9 \pm 2.6	10.9 \pm 2.4	9.7 \pm 1.5 \dagger	
100 kHz	12.0 \pm 1.8	7.8 \pm 2.7	14.1 \pm 4.00	14.5 \pm 2.9	11.2 \pm 2.1 \dagger	

Values are means \pm SD. BIA, bioelectrical impedance analysis; Sum, sum of arm, trunk, and leg. * Impedance of vectorial sum of arm, trunk, and leg. \dagger Phase of vectorial sum.

impedance index is directly proportional to the conducting volume and thus to the measured FFM. This investigation confirmed that at all frequencies and in all segments, there was a good correlation between the segmental FFM and the L^2 /impedance index (Fig. 3). Linear regression analysis in the prediction group is summarized in Table 3. On this basis, predicted FFM was calculated for each subject of the validation group at the three frequencies, and the residuals are plotted in Fig. 4. At 50 kHz, the mean difference (average of absolute values of the differences) between predicted and measured FFM was 2.26 ± 1.42 kg for the whole body, 0.30 ± 0.27 kg for the arm, 2.12 ± 1.89 kg for the trunk, and 0.61 ± 0.55 kg for the leg. Linear regression between segmental FFM and the L^2 /impedance index of the entire sample is also summarized in Table 3. It is noteworthy that, when performing linear regression analysis of these two parameters, a positive intercept of the regression line remains, indicating that part of the FFM measured by DEXA is not crossed by electrical current.

In a stepwise multiple regression model, we used independent variables such as weight, height, age, waist-to-hip ratio, percent ideal weight, and resistance index. We found that the latter had the best correlation to FFM ($r^2 = 0.62$), and the remaining variables improved r^2 by 7% ($r^2 = 0.69$). On the other hand, a model based on anthropometric variables only (weight, height, waist-to-hip ratio, and BMI) had an r^2 of 0.60.

The specific resistivity index was calculated by dividing the segmental FFM by the L^2 /impedance index and 1.1 g/cm^3 . This parameter expresses the resistance that could be measured between two $1 \times 1 \text{ cm}$ electrodes placed on the opposite side of a 1-g average FFM of the measured segment. When this parameter is low, it means that the FFM of that segment is a good conductor, whereas high values indicate FFM with higher insulating properties (Table 4). It must be stressed that

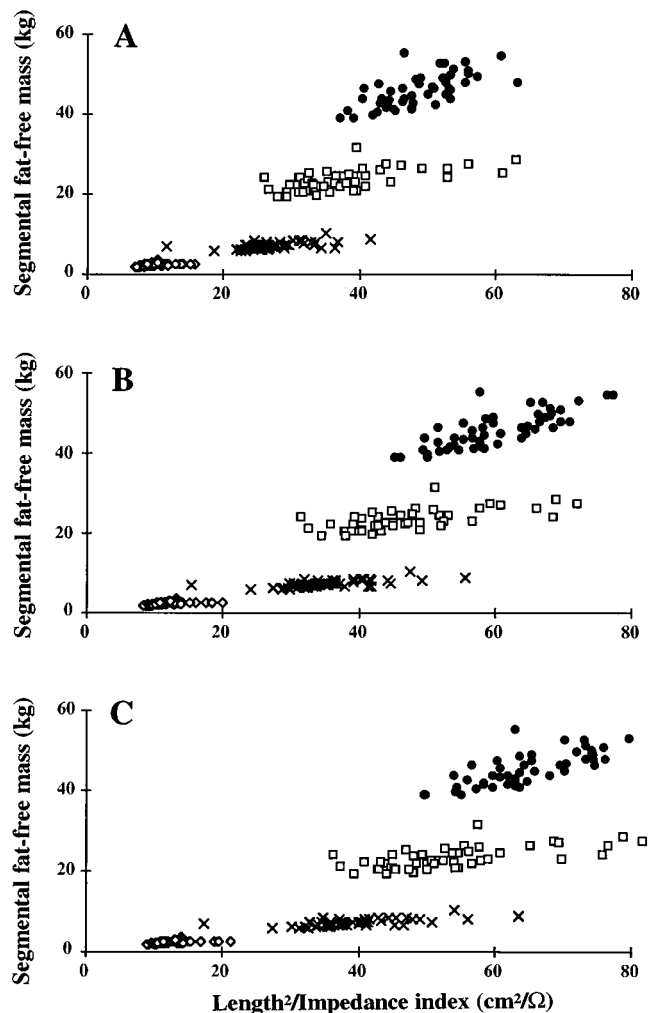


Fig. 3. Relationship between length (L)²/impedance index and FFM for whole body (\bullet) and for each segment [arm (\blacklozenge), trunk (\square), and leg (\times)] at 0.5 (A), 50 (B), and 100 (C) kHz.

Table 3. Equations between length²/impedance index and FFM

	Intercept, kg	Slope, kg Ω/cm ²	Error, kg	<i>r</i>
<i>Prediction group</i>				
Whole body				
0.5 kHz	22.6 ± 5.1	0.47 ± 0.10	3.3	0.62
50 kHz	19.1 ± 4.6	0.44 ± 0.08	3.0	0.71
100 kHz	18.0 ± 4.7	0.42 ± 0.07	3.0	0.72
Arm				
0.5 kHz	1.16 ± 0.34	0.096 ± 0.034	0.31	0.46
50 kHz	0.98 ± 0.32	0.095 ± 0.026	0.29	0.54
100 kHz	0.98 ± 0.32	0.090 ± 0.025	0.29	0.54
Trunk				
0.5 kHz	15.4 ± 1.8	0.211 ± 0.047	2.2	0.62
50 kHz	14.7 ± 1.9	0.184 ± 0.039	2.2	0.64
100 kHz	14.7 ± 1.9	0.160 ± 0.034	2.2	0.64
Leg				
0.5 kHz	5.8 ± 0.7	0.050 ± 0.025	0.66	0.33
50 kHz	5.5 ± 0.6	0.050 ± 0.019	0.63	0.41
100 kHz	5.5 ± 0.7	0.047 ± 0.017	0.63	0.42
<i>Whole sample</i>				
Whole body				
0.5 kHz	20.3 ± 3.5	0.52 ± 0.07	3.1	0.72
50 kHz	18.2 ± 3.1	0.46 ± 0.05	2.7	0.79
100 kHz	17.4 ± 3.2	0.43 ± 0.05	2.7	0.79
Arm				
0.5 kHz	1.21 ± 0.22	0.087 ± 0.021	0.29	0.50
50 kHz	1.17 ± 0.20	0.077 ± 0.017	0.28	0.55
100 kHz	1.15 ± 0.21	0.074 ± 0.016	0.27	0.56
Trunk				
0.5 kHz	15.8 ± 1.3	0.196 ± 0.035	2.1	0.62
50 kHz	15.9 ± 1.3	0.153 ± 0.028	2.1	0.62
100 kHz	16.1 ± 1.3	0.132 ± 0.24	2.1	0.62
Leg				
0.5 kHz	4.5 ± 0.6	0.101 ± 0.021	0.74	0.57
50 kHz	4.2 ± 0.5	0.088 ± 0.015	0.69	0.64
100 kHz	4.2 ± 0.5	0.077 ± 0.013	0.68	0.65

Values are means ± SD where indicated. FFM = intercept + slope × length²/impedance.

this parameter gives a crude estimation of specific resistivity, since it assumed that the measured segment was a homogeneous conductor.

DISCUSSION

This investigation, performed in lean and obese volunteers, demonstrated that segmental body composition could be determined by segmental BIA, compared with DEXA as a reference method. There was a significant correlation between segmental FFM obtained from BIA and FFM measured by DEXA. By using an appropriate anatomic location of electrodes, the recovery between the sum of the three segments and whole body BIA had an error of <1%.

Segmental body composition estimated by BIA. Several studies investigating segmental bioelectrical impedance have previously been published (1, 4, 5, 8, 9, 16–18, 21–23, 29). Unlike whole body BIA, which is well standardized (11), there are some differences between the various methods used and between the anatomic location of measured segments (18). All BIA devices did not measure the same value: some devices measure the impedance (Holtain device), whereas oth-

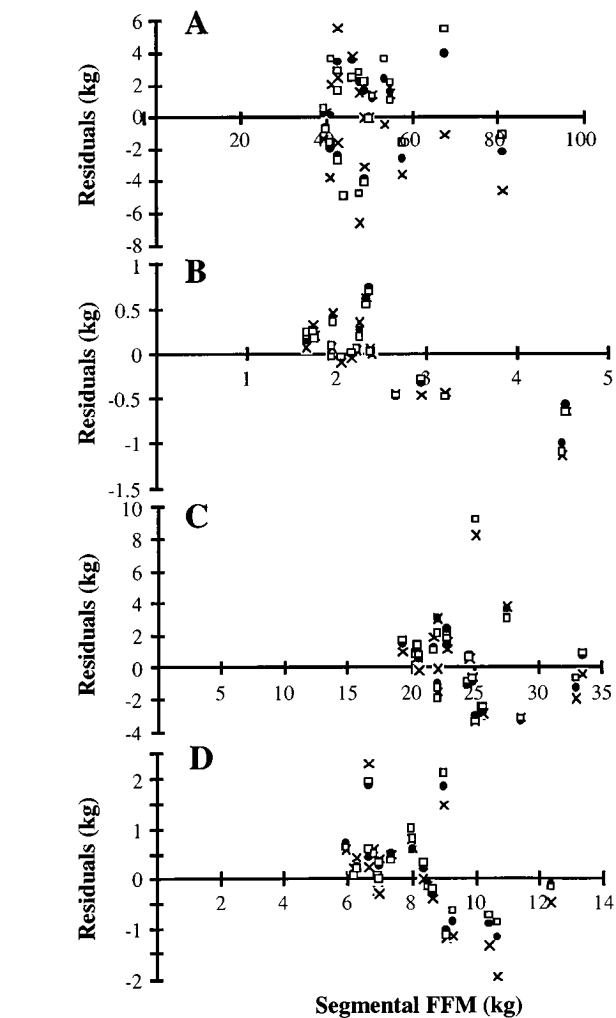


Fig. 4. Residuals of FFM validation group for whole body (A) and different segments [arm (B), trunk (C), and leg (D)] measured at 0.5 (x), 50 (●), and 100 (□) kHz.

ers measure resistance only (Valhalla device) and others measure both resistance and reactance, allowing calculation of impedance and phase shift (RJL, Xitron device). At low frequencies, phase shift is very low, so that the difference between the magnitude of resistance and impedance is of little practical importance, whereas at higher frequencies this difference cannot be neglected. When comparing resistance or impedance together, there is little difference between various BIA devices (8).

Table 4. Specific segmental resistivity indexes

	0.5 kHz	50 kHz	100 kHz
Whole body	857 ± 75	694 ± 55	636 ± 50
Arm	190 ± 29	159 ± 23	150 ± 21
Trunk	576 ± 88	457 ± 71	399 ± 63
Leg	248 ± 53	193 ± 39	172 ± 34

Values are means ± SD in Ω × cm. Within each frequency, all segments have significantly different specific segmental resistance, including arm vs. leg. Within each segment, specific resistance is significantly different for each frequency.

Table 5. Segmental BIA at 50 kHz measured by various investigators

Reference	Gender	Body	Arm	Trunk	Leg	Sum	%Body
<i>Resistance</i>							
Chumlea et al. (5)	M	474 ± 52	233 ± 24	80 ± 13	242 ± 27	544	117
Chumlea et al. (5)	F	588 ± 72	295 ± 39	86 ± 19	287 ± 35	688	114
Chumlea et al. (4)	M	476 ± 65	224 ± 26	83 ± 17	251 ± 29	558	117
Chumlea et al. (4)	F	601 ± 66	303 ± 38	93 ± 27	299 ± 34	695	116
Organ et al. (18)	M	455 ± 49	193 ± 27	37 ± 5	227 ± 26	457	100.4
Organ et al. (18)	F	594 ± 54	280 ± 31	51 ± 8	266 ± 25	597	100.5
Present study	F	460 ± 57	221 ± 36	45 ± 6	196 ± 25	463 ± 57	100.5 ± 1.9
<i>Reactance</i>							
Chumlea et al. (5)	M	59 ± 7	29 ± 4	15 ± 4	35 ± 7	78	131
Chumlea et al. (5)	F	65 ± 12	33 ± 8	13 ± 4	39 ± 8	84	129
Organ et al. (18)	M	58 ± 9	22 ± 4	6 ± 1	31 ± 5	58	101.7
Organ et al. (18)	F	67 ± 12	25 ± 6	7 ± 2	36 ± 7	68	101.4
Present study	F	78 ± 13	31 ± 8	10 ± 3	37 ± 6	75 ± 14	99.9 ± 7.8
<i>Impedance</i>							
Chumlea et al. (5)	M	478 ± 52	225 ± 24	81 ± 13	244 ± 27	550	115
Chumlea et al. (5)	F	591 ± 72	297 ± 38	88 ± 19	289 ± 35	673	114
Fuller and Elia (8)	M	532	251	62 ± 14	263	578	109
Fuller and Elia (8)	F	612	312	58	285	655	107
Stewart et al. (28)	M	447 ± 44	206 ± 20	68 ± 7	197 ± 23	471 ± 42	106
Stewart et al. (28)	F	553 ± 48	288 ± 28	86 ± 9	233 ± 23	607 ± 48	110
Present study	F	467 ± 58	223 ± 36	41 ± 5	200 ± 25	470 ± 58	100.5 ± 1.9

Values are means ± SD in Ω where indicated.

While performing segmental BIA, there are some methodological inconsistencies between the various investigators in the anatomic disposition of the current injecting and sensing electrodes (18). First, some investigators moved the current-injecting electrodes when measuring segmental impedance. Second, for measuring the leg impedance, some investigators (1, 4, 5) placed their sensing electrode at the anterior midline of the thigh, in the same plane as the gluteal crease, whereas others (8) placed the pelvic electrode at the same location as in the present study. Third, for measurement of the trunk, the upper sensing electrode was located at the sternal notch by some (8) and on the anterior part of the shoulder by others (1, 4, 5). Sensing-electrode location for the arm did not differ from one study to another. The anatomic location of the current-injecting electrode is of crucial importance because it determines the electrical current pathway across various segments of the body (18). In the majority of the previously published studies (1, 4, 5, 8), the current-injecting electrodes were moved and located just a few centimeters beneath the voltage-sensing electrodes. This changes the current pathways across the measured segment and thus the effective conducting volume measured. As shown in Table 5, in all studies where the current-injecting electrodes were moved (4, 5, 8, 28), the sum of segmental impedance (or resistance) was greater than the whole body impedance (resistance), whereas in the study of Organ et al. (18), where the electrodes were kept in place, the sum of segmental impedance perfectly corresponded to whole body assessments. In the present study, the degree of agreement between the sum of segmental impedance and whole body corresponded to the results of Organ et al. and was excellent. One critical issue is the relative

contribution of the trunk and legs to whole body impedance observed in different studies. In the former studies (4, 5, 8, 28), it ranged from 15 to 17% compared with ~10% in the study of Organ et al. and in the present investigation. The leg contributed to 50–53% of whole body resistance in studies where current-injecting electrodes were displaced compared with 43.0% in the present investigation. However, as shown by a positive intercept in the FFM vs. L^2 /impedance regression line, the volume assessed by segmental BIA was lower than the FFM measured by DEXA. In the trunk, for example, the electrical current flows from one shoulder to the ipsilateral thigh, and there is a limited amount of electrical current across the opposite shoulder and hip, although these tissues are included in DEXA-measured FFM.

Segmental equations for body composition by BIA derived from our sample are shown in Table 3. In each segment, there was a good agreement between FFM measured by DEXA and the index L^2 /impedance at all frequencies. However, at high frequencies (50 and 100 kHz in the present investigation), BIA assessment was more appropriate for FFM determination than at low-frequency BIA, since in the latter the electrically measured volume is primarily confined to the extracellular space. Despite the fact that this concept is not applicable for the whole body, Fig. 3 shows that there was a reasonable agreement between the height²/impedance index and FFM due to the fact that with increasing body size, the relative contribution of each segment to length and FFM rises in concert (Fig. 2). It must be stressed that the height/impedance index is the best single predictor of FFM, as measured by DEXA. The addition of other anthropometric variables

commonly used only slightly improved the prediction power.

Body composition assessed by DEXA. Since the advent of DEXA, the use of this device in body composition research has generated a great enthusiasm. The method is safe, requires little cooperation from the subject, and is totally independent, i.e., it does not have to be calibrated against a reference method. Moreover, DEXA devices are widely available for bone mineral content assessment in humans. Body composition investigation requires only software implementation. However, as any *in vivo* body composition assessment, it has nevertheless some limitations (24). For each pixel measured, two parameters are obtained (attenuation at low and high energy) and three variables need to be calculated (bone, lean, and fat). Mathematically, it is not possible to resolve a system composed of two equations with three unknown variables. Therefore, some assumptions have to be made. If the X-ray beam attenuation is high, the tissue crossed is assumed to contain bone; for this particular pixel, the system resolves the equations for bone and nonbone by assuming that the relative composition of nonbone is comparable to the surrounding bone-free (low-attenuation) pixels. This assumption implies that the composition of soft tissue overlying bone must have the same composition as the surrounding tissues. In addition, pixels including a small amount of calcium may be below the threshold value and may not be counted as bone but assimilated to very lean tissue. An additional interfering factor is the water content of FFM. Current DEXA software assumes that FFM contains 73.2% water. All of the subjects of our investigation were adults in good health (except obesity in some) with no concurrent medical conditions, and none were taking drugs. Whether the FFM of our sample did contain a fixed proportion of water (12) remains to be seen. DEXA remains a reliable technique for measuring body composition, but analysis of head and, to some extent, thorax soft tissue composition may be difficult because of superimposed bone. For the present investigation, there was a need for an independent technique capable of measuring segmental soft tissue composition. Some studies investigated limbs segmental body composition by anthropometry against BIA (4, 5, 8), but, to the best of our knowledge, only one investigation in humans has described segmental body composition assessed by DEXA vs. BIA (28).

When considering the values obtained by DEXA for body composition of the legs, trunks, and arms in this group of adults, there was a wide variation in segmental values. Therefore, it seems that the trunk acts as a reservoir for fat accumulation in overweight individuals. With increasing weight, the contribution of fat to excess body weight is as high as 86%, and about one-half of this adipose tissue is accumulated in the trunk.

In the present study, the relative error of FFM determination by BIA by using DEXA as the reference method was 6.7–7.6% for whole body, 15.9–16.9% for the arm, 11.7–12.9% for the trunk, and 11.9–12.7% for

the leg. This indicates the uncertainty of accurately assessing the absolute FFM in wide and short segments such as the trunk.

In conclusion, segmental body composition assessment by using segmental bioelectrical impedance constitutes a simple, inexpensive, and relatively accurate method to assess body composition in healthy and obese subjects. This study demonstrated that there is an excellent recovery between segmental and whole body BIA, with this highly standardized technique. Regression equations are provided that allow us to calculate segmental FFM by using segmental impedance and length. However, this requires prior standardization, particularly when different approaches and different BIA devices are employed.

The authors thank all of the subjects who participated in this investigation. We are indebted to K. Watrin and the radiology technicians who performed the DEXA scans and to Dr. M. Berger for reviewing the manuscript.

Address for reprint requests: Y. Schutz, Institute of Physiology, Faculty of Medicine, Rue du Bugnon 7, CH-1011 Lausanne, Switzerland.

Received 21 July 1995; accepted in final form 25 June 1996.

REFERENCES

1. Baumgartner, R. N., W. C. Chumlea, and A. F. Roche. Bioelectric impedance phase angle and body composition. *Am. J. Clin. Nutr.* 48: 16–23, 1988.
2. Bland, J., and D. Altman. Statistical methods for assessing agreement between two methods of clinical measurement. *Lancet* 1: 307–310, 1986.
3. Burgess, N. S. Wrestlers' minimal weight: anthropometry, bioimpedance, and hydrostatic weighing compared. *Med. Sci. Sports Exercise* 23: 247–253, 1991.
4. Chumlea, W. C., R. N. Baumgartner, and C. O. Mitchell. The use of segmental bioelectric impedance in estimating body composition. In: *Advances in In Vivo Body Composition Studies*, edited by S. Yasumura. New York: Plenum, 1990, p. 375–385.
5. Chumlea, W. C., R. N. Baumgartner, and A. F. Roche. Specific resistivity used to estimate fat-free mass from segmental body measures of bioelectric impedance. *Am. J. Clin. Nutr.* 48: 7–15, 1988.
6. Deurenberg, P., K. Van der Kooy, and J. G. Hautvast. Applications of bioelectrical impedance analysis: a critical review. *Basic Life Sci.* 55: 391–393, 1990.
7. Durnin, J. V. G. A., and M. Ramahan. The assessment of the amount of fat in the human body from measurements of skinfold thickness. *Br. J. Nutr.* 21: 681–689, 1967.
8. Fuller, N. J., and M. Elia. Potential use of bioelectrical impedance of the "whole body" and of body segments for the assessment of body composition: comparison with densitometry and anthropometry. *Eur. J. Clin. Nutr.* 43: 779–791, 1989.
9. Ishikawa, M., and N. Shinagawa. Nutritional assessment by bioelectrical impedance analysis. *Jpn. J. Clin. Med.* 49 Suppl.: 87–90, 1991.
10. Jebb, S. A., and M. Elia. Techniques for the measurement of body composition: a practical guide. *Int. J. Obes.* 17: 611–621, 1993.
11. Kushner, R. F. Bioelectrical impedance analysis: a review of principles and applications. *J. Am. Coll. Nutr.* 11: 199–209, 1992.
12. Lohman, T. Applicability of body composition techniques and constants for children and youth. *Exercise Sport Sci. Rev.* 14: 325–357, 1986.
13. Lukaski, H., W. Bolonchuk, C. Hall, and W. Siders. Validation of tetrapolar bioelectrical impedance method to assess human body composition. *J. Appl. Physiol.* 60: 1327–1332, 1986.
14. Lukaski, H., P. Johnson, W. Bolonchuk, and G. Lykken. Assessment of fat-free mass using bioelectrical impedance measurements of the human body. *Am. J. Clin. Nutr.* 41: 810–817, 1985.

15. **Mazess, R., H. Barden, J. Bisek, and J. Hanson.** Dual-energy X-ray absorptiometry for total-body and regional bone mineral and soft tissue composition. *Am. J. Clin. Nutr.* 51: 1106–1112, 1990.
16. **Mazess, R. B.** Alterations in body fluid content can be detected by bioelectrical impedance analysis. *J. Surg. Res.* 50: 461–468, 1991.
17. **Nyboer, J.** Workable volume and flow concepts of bio-segments by electrical impedance plethysmography. *Nutrition* 7: 396–408, 1991.
18. **Organ, L. W., G. B. Bradham, D. T. Gore, and S. L. Lozier.** Segmental bioelectrical impedance analysis: theory and application of a new technique. *J. Appl. Physiol.* 77: 98–112, 1994.
19. **Paijmans, I. J., K. M. Wilmore, and J. H. Wilmore.** Bioelectrical impedance analysis: a review of principles and applications. *J. Am. Coll. Nutr.* 11: 199–209, 1992.
20. **Pritchard, J. E., C. A. Nowson, B. J. Strauss, J. S. Carlson, B. Kaymakci, and J. D. Wark.** Evaluation of dual-energy X-ray absorptiometry as a method of measurement of body fat. *Eur. J. Clin. Nutr.* 47: 216–228, 1993.
21. **Rallison, L. R., R. F. Kushner, D. Penn, and D. A. Schoeller.** Errors in estimating peritoneal fluid by bioelectrical impedance analysis and total body electrical conductivity. *J. Am. Coll. Nutr.* 12: 66–72, 1993.
22. **Ross, R., L. Leger, P. Martin, and R. Roy.** Potential use of bioelectrical impedance of the “whole body” and of body segments for the assessment of body composition: comparison with densitometry and anthropometry. *Eur. J. Clin. Nutr.* 43: 779–791, 1989.
23. **Roubenoff, R., R. A. Roubenoff, L. M. Ward, S. M. Holland, and D. B. Hellmann.** Identifying body fluid distribution by measuring electrical impedance. *J. Trauma* 33: 665–670, 1992.
24. **Roubenoff, R. A., J. J. Kehayias, B. Dawson-Hughes, and S. B. Heymsfield.** Use of dual-energy X-ray absorptiometry in body composition studies: not yet a “gold standard.” *Am. J. Clin. Nutr.* 58: 589–591, 1993.
25. **SAS Institute.** *JMP Statistical Package for Macintosh* (3rd ed.). Cary, NC: SAS, 1994.
26. **Schutz, Y., and D. Bracco.** Impedance bioélectrique: utilité pour l'évaluation de la composition corporelle. *Méd. Hyg.* 51: 770–777, 1993.
27. **Segal, K., S. Burastero, A. Chun, P. Coronel, and R. Pierson.** Estimation of extra-cellular and total body water by multiple-frequency bioelectrical-impedance measurement. *Am. J. Clin. Nutr.* 54: 26–29, 1991.
28. **Stewart, S. P., P. N. Bramley, R. Heighton, J. H. Green, A. Horsman, M. S. Losowsky, and M. A. Smith.** Estimation of body composition from bioelectrical impedance of body segments: comparison with dual-energy X-ray absorptiometry. *Br. J. Nutr.* 69: 645–655, 1993.
29. **Zillikens, M. C., J. W. O. van den Berg, J. H. F. Wilson, and G. R. Swart.** Whole-body and segmental bioelectrical-impedance analysis in patients with cirrhosis of the liver: changes after treatment of ascites. *Am. J. Clin. Nutr.* 55: 621–625, 1992.

